16th World Conference on Earthquake, 16WCEE 2017

Santiago Chile, January 9th to 13th 2017

Paper N° 387 (Abstract ID)

Registration Code: S-U1461807168

Lateral force – story drift relationship of RC columns with side walls failing in flexure

D. Kato[(1)], T. Takamatsu[(2)] and Y. Komatsu[(3)]

[(1)] *Prof., Dr. Eng., Dept. of Architecture and Civil Engineering, Faculty of Engineering, Niigata University,dkato@eng.niigata-u.ac.jp*
[(2)] *Graduate Student, Graduate School of Science and Technology, Niigata University, f15e046j@mail.cc.niigata-u.ac.jp*
[(3)] *Graduate Student, Graduate School of Science and Technology, Niigata University, f16e042a@mail.cc.niigata-u.ac.jp*

Abstract

Practical use of secondary walls such as side wall is expected because contributions of secondary walls for stiffness or strength have been recognized. In this report hysteresis models of longitudinal reinforcing bars considering buckling and concrete considering confinement by not only transverse reinforcement but rigid base stub are proposed. Using these proposed models flexural analyses are conducted to simulate the moment - curvature relations of two RC column specimens with a side wall.

Authors have conducted static loading tests of 4 RC column specimens with an opened side wall failing in flexure and examined effects of openings on strength and deformation capacity of RC columns with a side wall. Specimens were subjected to constant axial load by two vertical jacks and lateral load reversals were applied at the top of the upper girder of the specimen. A flexural component among the lateral drift was evaluated using 6 sets of axial deformation obtained by vertical transducers installed at both sides of the specimen divided into 6 regions. Representative moment - curvature relationship, which would be compared with analysis in this study, was that obtained in the bottom region of the specimen.

Ramberg Osgood hysteresis model is used for stress-strain relationship of longitudinal reinforcing bars with some modification. The reversed Ramberg Osgood function is applied for stress-strain relationship after buckling. On the other hand a buckling model for longitudinal reinforcing bars of RC columns has been proposed taking buckling mode into account. In general buckling length of longitudinal reinforcement in RC members extends over several times of the spacing of the transverse reinforcement. The buckling mode represents the number of hoop spacing along one buckling wave form.

Authors have proposed a model of stress-strain relationship of concrete confined by hoop reinforcement. However authors have also reported that real flexural behaviors of columns could not be simulated with enough accuracy using the concrete model confined by hoop reinforcement only. This was because the compressive failure zone of concrete was limited locally near critical sections in case of columns subjected to moment and shear force and the confinement for concrete from rigid base stubs could not be ignored. From this view point confinement from rigid base stub is considered.

The analytical cases ignoring both buckling of main bars and confinement from rigid base stub indicate that the analytical results cannot simulate the test results well from following two view points; i.e. (i)calculated restoring force after maximum strength decreases rapidly comparing to test in the positive loading direction where side wall is subjected to compressive force. (ii)Calculated hysteresis energy becomes high comparing to test in the negative loading direction where side wall is subjected to tensile force. On the other hand the cases considering both buckling of main bars and confinement from rigid base stub indicate that the analytical results can simulate the test results qualitatively well from following two view points; i.e. slope after maximum strength in the positive loading direction and hysteresis energy in the negative loading direction.

Keywords: buckling of bars; confinement by transverse reinforcement; reinforced concrete; flexural analysis

1. Introduction

Practical use of secondary walls such as side wall is expected because contributions of secondary walls for stiffness or strength have been recognized[1)]. Authors have conducted static loading tests of 4 RC column specimens with an opened side wall failing in flexure and examined effects of openings on strength and deformation capacity of RC columns with a side wall[2)3)].

Behavior of RC columns with side walls failing in flexure deeply depends on characteristics of concrete and longitudinal reinforcing bars arranged near the edge of side walls because the maximum strength and deformation capacity are determined by compressive failure of elements located near the edge of side walls in general. Furthermore buckling of longitudinal reinforcing bars located near the edge is apt to occur due to subjected cyclic high strain which leads to the degradation of tensile stress. In case of columns with one side wall on one side of the column the above mentioned two effects occur in independent loading directions separately. In other words columns with a side wall can be good analytical objects to examine the effect of compressive concrete of side wall subjected to compression on deformation capacity and the effect of stress degradation of longitudinal reinforcing bars on strength.

In this report hysteresis models of longitudinal reinforcing bars considering buckling and concrete considering confinement by not only transverse reinforcement but rigid base stub are proposed. Using these proposed models flexural analyses are conducted to simulate the moment - curvature relations of two RC column specimens with a side wall, which are selected from above mentioned 4 specimens from the view point that openings have no influence on their behavior.

2. Outline of tests and objective moment-curvature relationship

Table 1 shows properties of objective two specimens. Fig. 1 shows their arrangement and loading setup. Main variation was the width of side walls other than a little difference of material strength. Specimens were subjected to constant axial load by two vertical jacks and lateral load reversals were applied at the top of the upper girder of the specimen, the height of which was 1300mm from the critical section of the specimen. Note that additional moment was applied to specimens by two vertical jacks, which lead to the enhancement of shear span from 1300mm to 1500mm. Lateral drift angle in this report was represented by lateral deformation observed by the transducer located at the loading point divided by the height (1300mm) of the loading point. On the other hand a flexural component among the lateral drift was evaluated using 6 sets of axial deformation obtained by vertical transducers installed at both sides of the specimen divided into 6 regions in each side shown in Fig. 1(a). Representative moment - curvature relationship, which would be compared with analysis in this study, was that obtained in the bottom region of the specimen (region 6, the height was 100mm).

Confinement to concrete provided by an elastic region of specimens and a rigid base stub adjacent to the hinge region of the specimens is considered in this study as shown later. Because the confinement depends on the height of the compressive failure zone of concrete, it is necessary to evaluate the height. In this study the height h_p is estimated by Eq. (1) using experimental data. Eq. (1) represents a simplified equation showing the relationship between flexural component of lateral drift angle R_f at the loading point and curvature of the critical section ϕ_B on the assumption that the curvature inside the height h_p is constant and other zones are rigid. Fig. 2 shows the relationship between the flexural component of lateral drift angle at the loading point (R_f) and the estimated height of compressive failure zone (h_p) calculated using Eq.(1) for every loading step. Note that the data of the final loading cycle of specimen CSWO-F-100U is not shown because one of the transducers got off during the loading.

$$h_p = R_f / \phi_B \tag{1}$$

where, R_f denotes a flexural component of lateral drift angle at the loading point obtained using axial deformation given by above mentioned 6 sets of transducers. ϕ_B denotes a curvature at the bottom section of the specimen (region 6).

Fig. 2 indicates that the value of estimated height of compressive failure zone converges toward certain value with the increasing value of lateral drift angle although plots highly scatter in a small range of drift angle. The converged values of estimated height of compressive failure zone are found to be 140mm for specimen CSWO-F-U and 170mm for specimen CSWO-F-100U considering values of positive loading direction, in which side walls are subjected to compressive force.

Table 1 – Properties of specimens[2)3)]

specimen		CSWO-F-U[2)]	CSWO-F-100U[3)]
column section (mm)		250×250	
side wall section (mm)		75×500	100×500
height of column (mm)		1000	
shear span (mm)		1500	
(shear span ratio)		(2.0)	
main bar of column	arrangement	4-D13	
	yield strength (N/mm^2)	396	377
hoop of column	arrangement (ratio, %)	2-D6@50(0.512)	
	yield strength (N/mm^2)	309	403
reinforcement of side wall (ver.&hor.)	arrangement (ratio, %)	2-D6@100	
		(0.85)	(0.64)
	yield strength (N/mm^2)	309	403
end bar of side wal (vertical)	arrangement	1-D10	
	yield strength (N/mm^2)	369	382
opening	height (mm)	150	
	lengh (mm)	150	
	location	center	
concrete strength (N/mm^2)		20.7	22.4
axial load (N)		400,000	

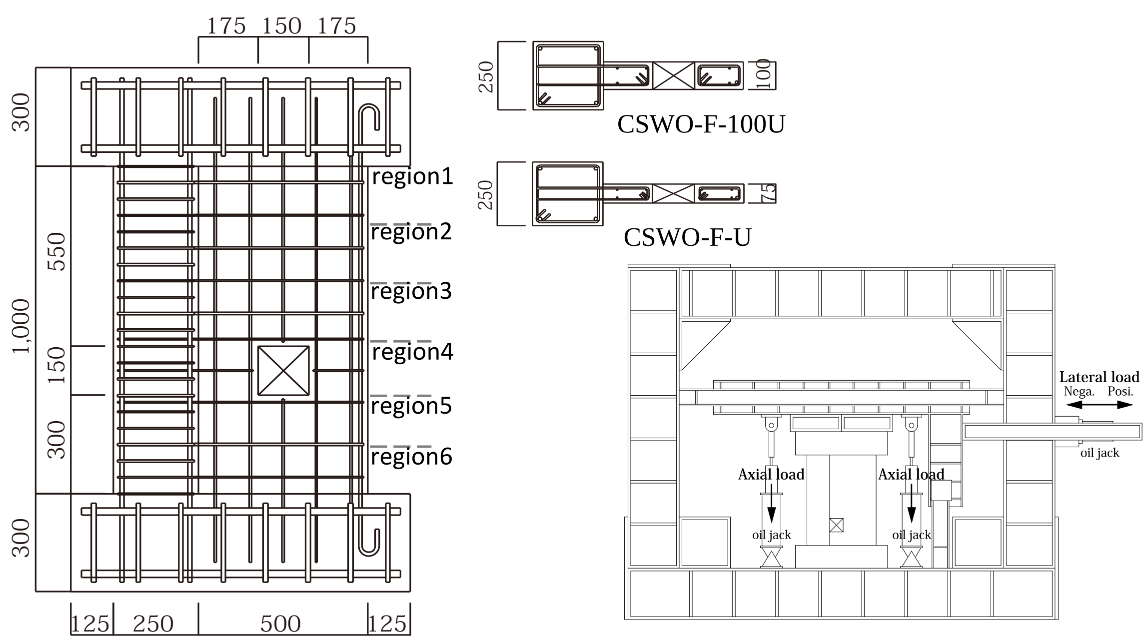

(a)Arrangement of reinforcement of specimens (b)Loading setup

Fig. 1– Outline of test[2)3)]

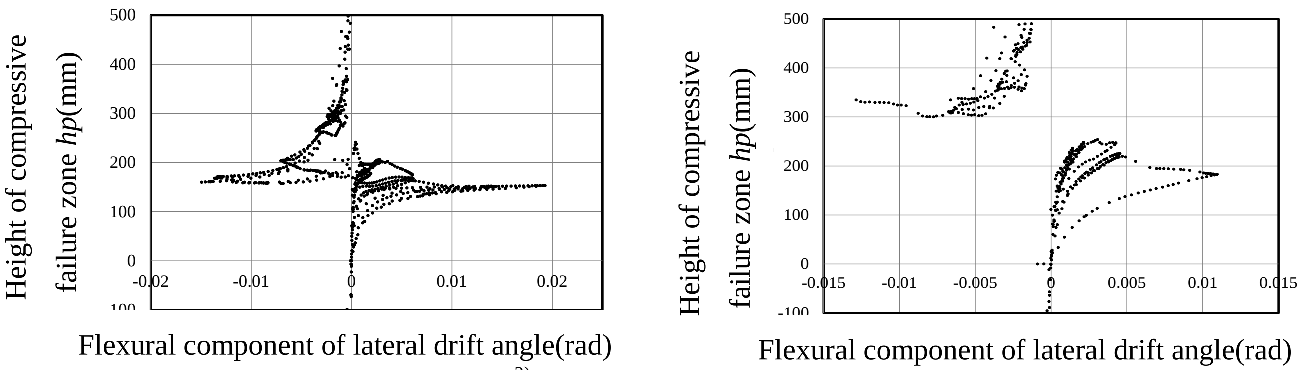

(a)specimen CSWO-F-U[2)]　　(b)specimen CSWO-F-100U[3)]

Fig. 2 – Estimation of height of compressive failure zone of concrete

3. Model of longitudinal reinforcement considering buckling

3.1 Stress strain relationship of longitudinal reinforcement

Ramberg Osgood hysteresis model[4)] is used for stress-strain relationship of longitudinal reinforcing bars with some modification. Fig. 3(a) shows cyclic rules of the model. The parameter γ of this function is assumed to be 8 according to Ref. 4), in which the value of γ equals to be 5 ~ 10 was suggested for main longitudinal bars. On the other hand the parameter η, which is a coefficient to determine the strain at starting point of strain hardening, is counted backward by evaluated strain at starting point of strain hardening (ε_{ER}) shown later.

Fig. 3(b) shows the backbone curve after buckling, in which the reversed Ramberg Osgood function is applied. The reversed curve is determined by a strain at starting point of buckling (d_1) and a strain when the stress becomes 0 (d_3) as shown in Fig. 3(b). It is added that the evaluating method of d_1 and d_3 are shown in Subsection 3.2. Fig. 3(c) shows an example of hysteresis under cyclic loading, the main rules of which are as follows;

(i)In case of cyclic loading buckling occurs when accumulated compressive strain reaches the buckling strain proposed for monotonic loading (ε_{BUC}).

(ii)Hysteresis rules after buckling yield to the rules before buckling shown in Fig. 3(a).

(iii)Oriented point after unloading is the past maximum response point in the opposite loading direction. After buckling, however, the stress of the oriented point should be less than the stress at unloading point.

(iv)After the stress becomes less than 0 on the reversed buckling curve, the stress hereafter should be kept 0.

(v)Independent of buckling the stress should be kept 0 after accumulated tensile strain reaches the rupture strain set for monotonic loading (ε_{RUP}).

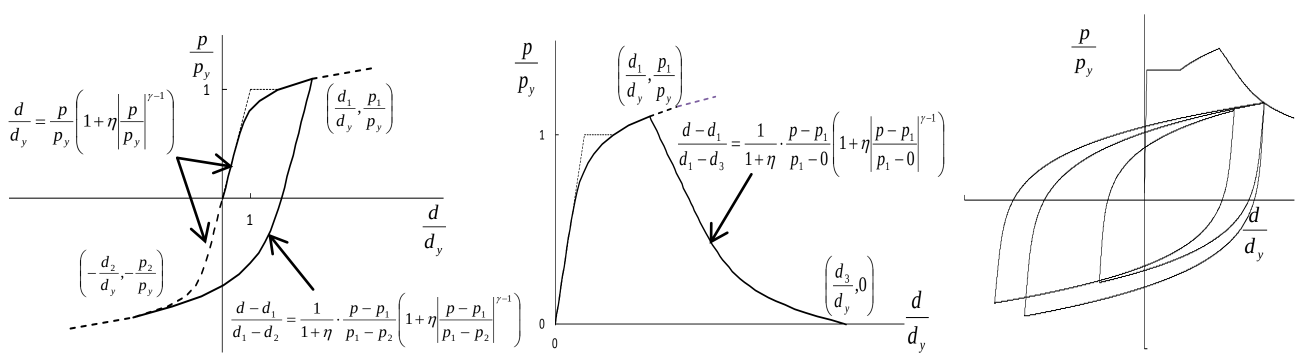

(a)Hysteresis rule for cyclic loading[4)]　　(b)Backbone curve after buckling　　(c)Examle of cyclic loading

Fig. 3 – Stress-strain hysteresis model for longitudinal bars according to Ramberg Osgood model

3.2 Evaluating method of buckling strain of bars subjected to monotonic loading

A buckling model for longitudinal reinforcing bars of RC columns has been proposed taking buckling mode (N_B) into account in Ref. 5). Fig. 4(a) shows the concept of the buckling behavior, which represents an example of buckling mode of 3. In general buckling length of longitudinal reinforcement in RC members extends over several times of the spacing of the transverse reinforcement. The buckling mode represents the number of hoop spacing along one buckling wave form.

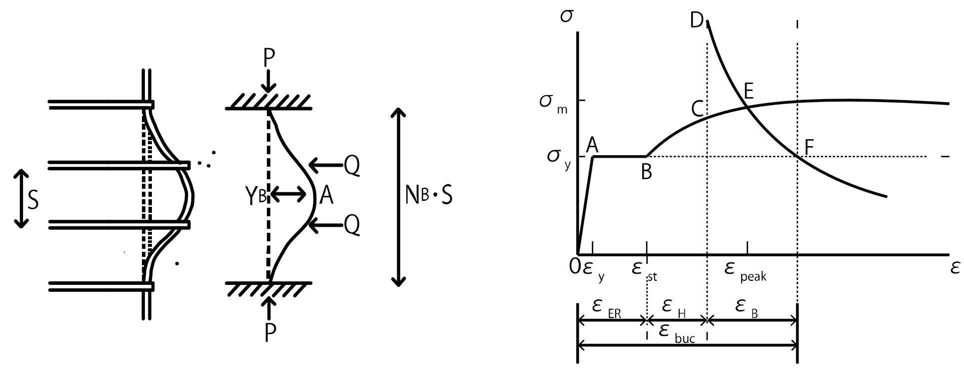

(a)Concept of buckling behavior (Example in case of N_B=3)

(b)Stress-strain relationship after buckling

Fig. 4 –Evaluating method of stress-strain relationship of longitudianl bars after buckling[5)]

Fig. 4(b) shows stress-strain relationship after buckling under monotonic loading and the strain at point F is defined as buckling strain (ε_{BUC}). Using this model the buckling strain of a longitudinal bar can be expressed by Eq. (2). Note that Eq. (2) depends on the buckling mode (N_B) which means that the buckling strain can be given as the minimum among the values calculated for the possible buckling modes.

$$\varepsilon_{BUC}(N_B) = \varepsilon_{ER} + \varepsilon_H(N_B) + \varepsilon_B(N_B) \tag{2}$$

$$\varepsilon_{ER} = -1.45 \cdot \varepsilon_y + 0.026$$

$$\varepsilon_H(N_B) = 1.4 \frac{\phi_h}{N_B \cdot (\frac{S}{2})} - 0.29 \qquad (\geq 0)$$

$$\varepsilon_B(N_B) = \left(\frac{2}{3 \cdot N_B \cdot a_x \cdot \alpha} \cdot \left(\gamma_1 \cdot g(N_B) - 1 \right) \right)^2$$

$$g(N_B) = 1 + \frac{\pi \cdot a_x \cdot f(N_B) \cdot N_B \cdot \alpha \cdot \beta^2 \cdot \gamma_2}{16}$$

$$f(N_B) = \begin{cases} \dfrac{(N_B{}^2 - 1)}{N_B} & (N_B:\ \text{odd number}) \\ \dfrac{(N_B{}^2 + 2)}{N_B} & (N_B:\ \text{even number}) \end{cases}$$

where, $\alpha = S/\phi_h$, $\beta = \phi_{we}/\phi_h$, $\gamma_1 = \sigma_m/\sigma_y$, $\gamma_2 = \sigma_{wye}/\sigma_y$, a_x=0.65. σ_y, ε_y, σ_m and ϕ_h denote the yielding stress, yielding strain, maximum stress and diameter of the longitudinal reinforcing bar. S, ϕ_{we} and σ_{wye} denote spacing, effective diameter and effective yielding stress of the transverse reinforcing bar to confine longitudinal reinforcing bars. Where, effective diameter denotes an average diameter of a group of outside hoop type reinforcing bars and intermediate tie bars, which show different confining effects. And effective yielding stress represents degradation of effectiveness of transverse reinforcement in case of high strength bars. These are expressed as follows.

$$\phi_{we} = \phi_w \cdot \sqrt{\frac{2 + \nu \cdot m}{2 + n}}$$

$$\sigma_{wye} = 20\sqrt{\sigma_{wy}} \qquad (\leq \sigma_{wy}) \qquad \text{(unit: N/mm}^2\text{)}$$

where, σ_{wy} denotes yielding stress of the transverse reinforcement. n denotes the number of longitudinal bars except for corner bars and m denotes those confined by intermediate bars among n. ν represents effectiveness factor of intermediate tie bars to outside hoop type bars and the value of 2.2 was proposed in Ref. 6).

It must be added that the strain at starting point of buckling (d_1 shown in Fig. 3(b)) is given by buckling strain ε_{BUC} (point F in Fig. 4(b)) in this study ignoring the difference of the strain between point E and F although starting point of buckling d_1 represents the point E essentially. Furthemore, the strain when the stress becomes 0 (d_3 shown in Fig. 3(b)) is assumed to be given as follows to match the proposed model with original buckling model by Ref. 5). Fig. 5 shows backbone curves of three longitudinal reinforcing bars used for specimen CSWO-F-U indicating that the proposed models are comparable with original models. Note that the replaced Ramberg Osgood models in Fig. 5 represent unpractical functions which are obtained to match the strain d_1 with the strain at point E by trial and error method.

$$d_1 = \varepsilon_{BUC}(N_B), \qquad d_3 = 20 \cdot \varepsilon_{BUC}(N_B)$$

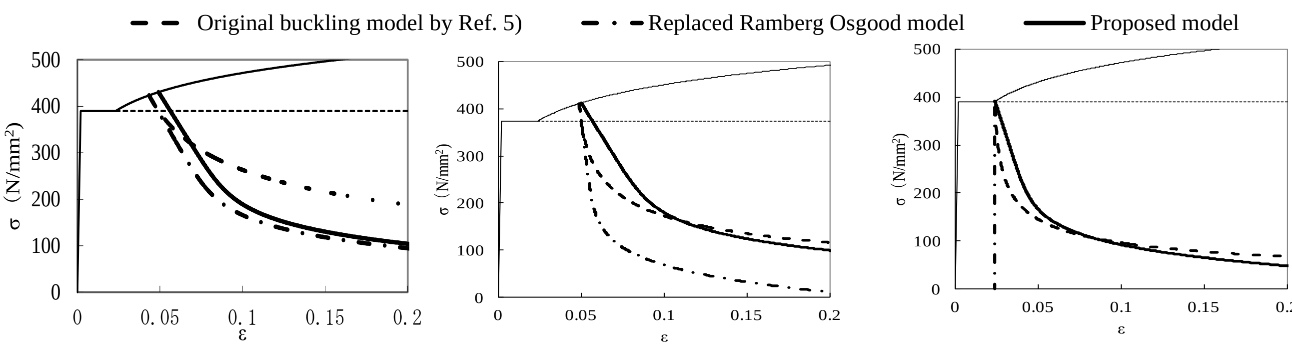

(a)Main bars of columns (D13, N_B=3)

(b)Vertical edge bars of side walls (D10, N_B=1)

(c)Vertical bars of side walls (D6, N_B=1)

Fig. 5 –Evaluated stress-strain relationship of longitudianl bars (examples of specimen CSWO-F-U2))

4. Model of concrete considering confinement from reinforcement and rigid base stub

4.1 Model of concrete confined by transverse reinforcement

Authors have proposed a model of stress-strain relationship of concrete confined by hoop reinforcement in Ref. 7). The model can be summarized as follows.

(i)Details of reinforcing arrangement such as hoop spacing or hoop diameter can be taken in account because mechanism of confinement by hoop reinforcement is different from that by hydraulic pressure, which means that the confining effects depend on arrangement details.

(ii)Axial strain of the model represents that within the failure zone of concrete only because observed experimental data on axial strain were examined separating them into 2 parts; i.e. strain in damaged zone and others.

(iii)Behavior after maximum stress of the model is expressed by bi-linear relationship; i.e. the steep falling branch and the following stable flat portion.

Fig. 6(a) shows a backbone curve of the proposed confined concrete model, the maximum stress σ_{cp}, the strain at the maximum stress ε_{cp} and the slope of falling branch E_{up} are given by Eqs. (3)~(5) depending on the effective confining stress σ_{tp} from transverse reinforcement. σ_{b1} and σ_{b2} are confining stresses from a rigid base stub shown later in Subsection 4.2. Note that units used in this report are N and mm.

$$\sigma_{cp} = \sigma_c + 4.1 \cdot (\sigma_{tp} + \sigma_{b1}) \tag{3}$$

$$\varepsilon_{cp} = \varepsilon_c + 0.0015 \cdot (\sigma_{tp} + \sigma_{b1}) \tag{4}$$

$$E_{up} = \frac{E_u}{1 + 12.6 \cdot (\sigma_{tp} + \sigma_{b2})} \tag{5}$$

$$\sigma_{tp} = \frac{\varepsilon_c}{\frac{2.8 + 0.0035 \cdot {}_eK_{cf}}{K_{cf}} - 0.0015} \qquad (0 \le \sigma_{tp} \le \sigma_{tup}) \cdot \qquad K_{cf} = \frac{a_w \cdot E_s}{B_c \cdot S}$$

$${}_eK_{cf} = K_{cf} \cdot \sqrt{\frac{S}{\min(D_c, B_c)}} \cdot (\frac{1}{N_{BUN}{}^2})$$

where, a_w , S and E_s denote the sectional area, the spacing and the the modulus of elasticity of a set of the hoop reinforcement. D_c and B_c denote the core depth and width of the section. N_{BUN} denotes the number of core regions divided by tie of the section (N_{BUN} =1 for peripheral hoop reinforcement, N_{BUN} =2 for hoop with one tie reinforcement). And σ_c, ε_c and E_u denote the maximum strength, strain at the maximum strength and the slope of the falling branch of concrete confined by neither hoop reinforcement nor rigid base stub, which are given as follows. Note that Eqs. (3)~(5) can be also used for concrete confined by rigid base stub only.

$$\sigma_c = 0.85 \cdot \sigma_B, \qquad \varepsilon_c = 13.7 \cdot 10^{-6} \cdot \sigma_c + 0.00169$$

$$E_u = \frac{\sigma_c - 10}{\varepsilon_c - 0.005}$$

Where, σ_B denotes the compressive strength of concrete.

Furthermore, σ_{tup} which means the upper limit of confining stress σ_{tp} is given by following Equations.

$$\sigma_{tup} = \frac{a_w \cdot \sigma_{wy}}{D_c \cdot S} \cdot \frac{\frac{2}{1 + C_0} + N_{BUN} - 1}{N_{BUN} + 1}$$

$$C_0 = (\frac{1}{20}) \cdot (\frac{D_c}{\phi_w}) \cdot \gamma$$

$$\gamma = 0.0005 \cdot \sigma_{wy} \qquad (\le 2)$$

where, ϕ_w and σ_{wy} denote the diameter and the yielding stress of the hoop reinforcement.

Furthermore, the stable flat stress σ_{up} after steep falling branch is given by Eq. (6).

$$\sigma_{up} = \sigma_{tup} \cdot \frac{\sin\theta \cdot \cos\theta + \mu \cdot \sin\theta \cdot \sin\theta}{\sin\theta \cdot \cos\theta - \mu \cdot \cos\theta \cdot \cos\theta} \tag{6}$$

where, θ denotes the inclination angle of the crack,which is assumed to be 45° in this study. And μ denotes the coefficient of friction given as follows.

$$\mu = 0.32 + 0.0064 \cdot \sigma_c$$

On the other hand, popular hysteresis rules of concrete shown in Ref. 8) is used, the point of which is that the oriented point after unloading from tensile loading direction is the past maximum response point of compressive loading direction.

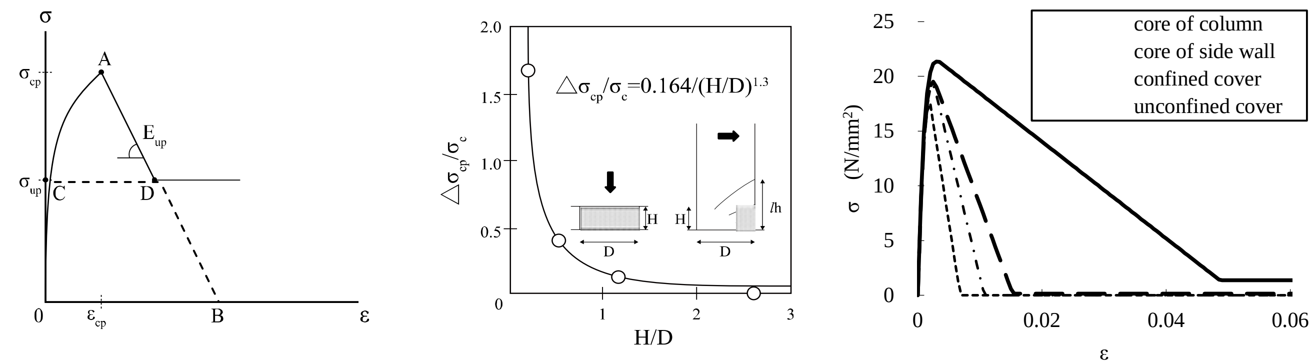

(a) Stress-strain relationship[7)] (b)Confinement from rigid base stub (c)Evaluated σ–ε curve

(Example of specimen CSWO-F-U[2)])

Fig. 6 –Stress-strain relationship of confined concrete

4.2 Model of concrete confined by rigid base stub

In Ref. 8) authors have reported that real flexural behaviors of columns could not be simulated with enough accuracy using the concrete model confined by hoop reinforcement shown in Subsection 4.1 only. This was because the compressive failure zone of concrete was limited locally near critical sections in case of columns subjected to moment and shear force and the confinement for concrete from rigid base stubs could not be ignored. Fig. 6(b) shows the relationship between aspect ratios of uni-axial loaded mortar specimens, which are defined as height(H) divided by depth(D) of the specimen, and the enhancement ratios of maximum axial stress using the data reported in Ref. 9). A solid curved line in Fig. 6(b) represents formulation showing this phenomenon. Furthermore replacing height(H) and depth(D) of uni-axial specimen by height of compressive failure zone of concrete(h_p) and width of side wall(t_w) of objective column specimens with a side wall, confining stress for maximum stress (σ_{b1}) used in Eq. (3) can be given as follows. Note that confining stress σ_{b2} from rigid base stub to the falling branch of stress- strain relahionship is given according to Ref. 8).

$$\sigma_{b1} = \frac{1}{4.1} \cdot \sigma_c \cdot \frac{0.164}{(H/D)^{1.3}} \qquad \left(= \frac{0.04 \cdot \sigma_c}{(h_p / t_w)^{1.3}} \right)$$

$$\sigma_{b2} = 0.1 \cdot \sigma_{b1}$$

where, h_p denotes the height of compressive failure zone estimated as 140mm for specimen CSWO-F-U and 170mm for specimen CSWO-F-100U in Section 2. t_w denotes width of the side wall (75mm, 100mm).

5. Analytical results

5.1 Application method of proposed models

Flexural analysis is conducted on the assumption that a section remains plane after bending (Fiber Model) for representative observed moment - curvature relationship, which was obtained in the bottom region of the specimen (region 6, the height was 100mm). Existence of openings is ignored in the analysis. Longitudinal reinforcing bars are classified into 3 groups, i.e. main bars of columns, vertical edge bars of side walls and vertical bars in side walls (see Fig. 5). The sum of the gross sections of each group is arranged at the center of the group. Gross section of concrete is divided to about 25mm square elements. These elements are classified into 3 groups; i.e. core concrete of column confined by hoop reinforcement, core concrete of side wall confined by horizontal reinforcement and cover concrete confined by rigid base stub only. Note that the sectional area of core is defined as the area surrounded by the center of confining reinforcing bars.

Evaluated stress-strain relationship of three groups of bars of specimen CSWO-F-U are shown in Fig. 5(a)~(c) with the value of buckling mode N_B. Note that the buckling mode of column main bars only is 3 although that of others is 1. Assumptions for application on longitudinal bars are as follows.

(i)For main bars (D13) of columns confined by only peripheral hoop type reinforcement (D6), the method shown in Subsection 3.2 are applied with the value of n=0 and m=0. (In other words the D13 bar is confined by one D6 bar.)

(ii)For vertical edge bars (D10) of side walls confined by horizontal reinforcing bars of side wall (D6), the D10 bar is assumed to be confined by one D6 bar.

(iii)For vertical bars in side walls (D6) because total number of 10 bars are confined by rectangular hoop type transverse reinforcement (D6), only 4 of them are assumed to be effectively confined which lead to the effectiveness factor of 0.4. (In other words the D6 bar is confined by 40% of D6 bar.)

(iv)The rupture strain for monotonic loading (ε_{RUP}) is assumed to be 0.3.

Evaluated stress-strain relationship of three groups of concrete of specimen CSWO-F-U are shown in Fig. 6(c) comparing with the behavior of unconfined concrete. Assumptions for application on concrete are as follows.

(i)For core concrete of column confined by hoop reinforcement, the method shown in Subsections 4.1 and 4.2 are applied directly, where observed values of 140 or 170mm are used as h_p to evaluate the confining stress $\sigma_{b1,2}$ from rigid base stub.

(ii)For core concrete of side wall confined by flat type horizontal side wall reinforcement, because the confining effect by side wall reinforcement to orthogonal direction is much lower comparing to that to plane direction, the imaginary section of 500mm×500mm square section is assumed to evaluate the confinement.

(iii)For cover concrete confined by rigid base stub only, confining stress $\sigma_{b1,2}$ from rigid base stub is applied.

5.2 Examples of analytical results

Figs. 7(a)(b) show observed moment-curvature relationship of two specimens comparing with analytical results. Note that the data of the final loading cycle of specimen CSWO-F-100U is not shown because of the measurement trouble. Figs. 7(a-1)(b-1) show the analytical case ignoring both buckling of main bars and confinement from rigid base stub, which indicate that the analytical results cannot simulate the test results well from following two view points. (i)Calculated restoring force after maximum strength decreases rapidly comparing to test in the positive loading direction where side wall is subjected to compressive force. (ii)Calculated hysteresis energy becomes higher comparing to test in the negative loading direction where side wall is subjected to tensile force.

On the other hand Figs. 7(a-2)(b-2) show the case considering both buckling of main bars and confinement from rigid base stub, which indicate that the analytical results can simulate the test results qualitatively well from following two view points; i.e. slope after maximum strength in the positive loading direction and hysteresis energy in the negative loading direction.

However from the quantitative view point following two problems can be commented for future study. (i)A gap of restoring force between calculation and observation at peak point of each cycle in the negative loading direction cannot be negligible, which depends on the hysteresis model of longitudinal reinforcement after buckling. (ii)Oriented point after unloading from negative loading direction is the past maximum response point in the positive loading direction in calculation although observed restoring force of oriented point degrades, which depends on the cyclic rules of hysteresis model of concrete.

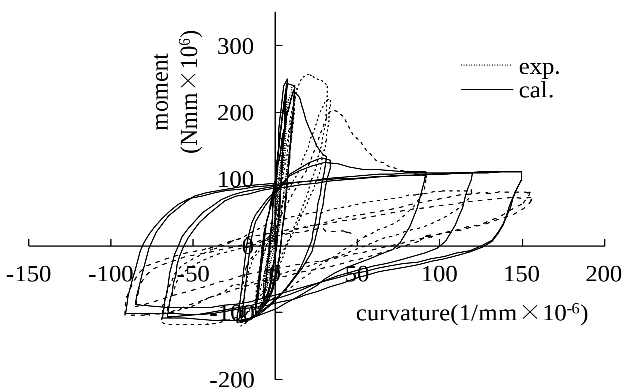

(a-1) Ignoring buckling and confinemen from rigid base stub

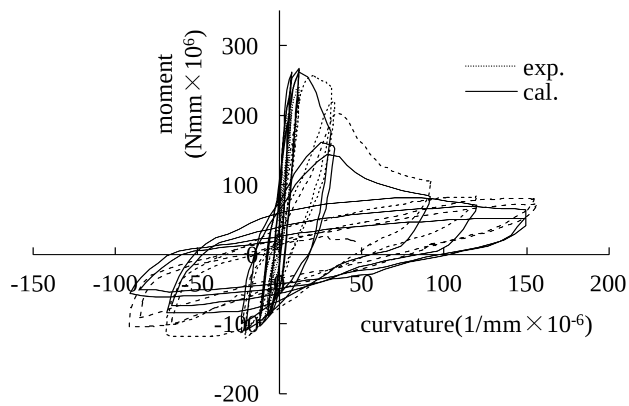

(a-2) Considering buckling and confinement from rigid base stub

(a)specimen CSWO-F-U[2)]

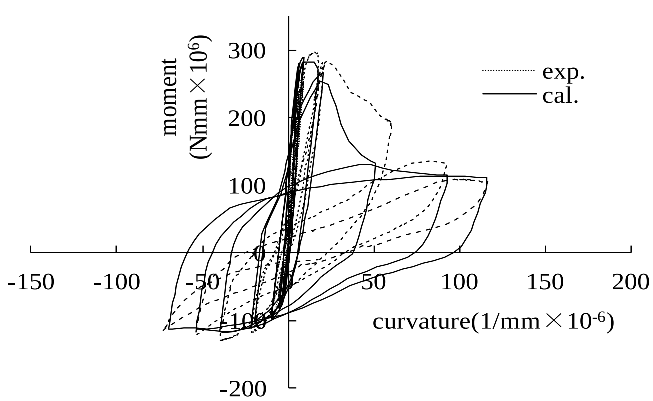

(b-1) Ignoring buckling and confinemen from rigid base stub

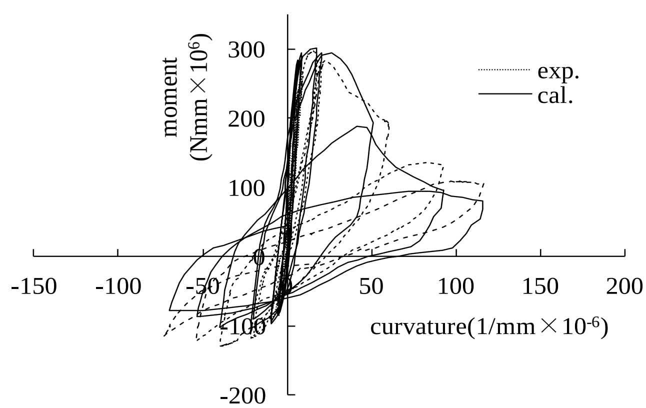

(b-2) Considering buckling and confinement from rigid base stub

(b)specimen CSWO-F-100U[3)]

Fig. 7 –Comparison of moment-curvauture relationship between experiment and analysis

6. Conclusions

(1)Hysteresis models of longitudinal reinforcing bars considering buckling and concrete considering confinement by not only transverse reinforcement but rigid base stub are proposed.

(2)Flexural analyses are conducted using proposed models to simulate the moment - curvature relations of RC column specimens with a side wall, which indicate that the analytical results can simulate the test results qualitatively well

(3)However from the quantitative view point improvement of hysteresis model of longitudinal reinforcement after buckling and cyclic rules of hysteresis model for concrete is required.

7. References

[1] Daisuke KATO, Masahide KOBAYASHI, Tadashi TAKAMATSU and Kenichi OSHIO : STUDY ON DAMAGED RC SCHOOL BUILDINGS PAYING ATTENTION TO COLUMNS WITH SIDEWALLS, Journal of Structural and Construction Engineering, Architectural Institute of Japan, Vol.80,No.718, pp.1931-1939, 2015.12 (in Japanese)

[2] Tetsuo Watanabe, Takaya Nakamura, Ryoichi Tamura and Daisuke Kato, Static Loading Tests of R/C Columns with a side wall failing in flexure, Proceedings of the Japan Concrete Institute, Vol.36, No.2, 2014, pp283-288 (in Japanese)

[3] Tadashi Takamatsu, Tetsuo Watanabe, Ryoichi Tamura and Daisuke Kato, Expeimental study on effects of position of openings on flexural behavior of R/C Columns with a side wall, Proceedings of the Japan Concrete Institute, Vol.37, No.2, 2015, pp.115-120 (in Japanese)

[4] Jennings,P.C., Response of Simple Yielding Structures to Earthquake Excitaion, Ph.D. Thesis, California Institute of Technology, Pasadena, 1963

[5] Kato, D., Kanaya, J. and Wakatsuki, K., Buckling Strains of Main Bars in Reinforced Concrete Members, Proceedings of the fifth East Asia-Pacific Conference on Structural Engineering and Construction, Volume 1, 1995, pp.699-704

[6] Ooya, H. and Kato, D. , Experimental Study on Buckling Behavior of Intermediate Longitudinal Bars in R/C Members, Transactions of the Japan Concrete Institute, Vol. 16, 1994, pp. 365-372

[7] D.Kato, F.Watanabe, M. Nishiyama and H. Sato, "Confined Concrete with High-strength Materials," High-Strength Concrete(HSC) in Seismic Regions,SP-176, America Concrete Institute, 1998, pp.85-104

[8] KATO, D., Ductility of Reinforced Concrete Columns with Various Reinforcing Arrangements, the 10-th World Conference on Earthquake Engineering, 1992, Vol.5, pp.3029-3034

[9] Yoshio Kosaka and Yasuo Tanigawa, Physical characteristics of mortal confined by hoop, Summaries of technical papers of annual meeting, Architecture Institute of Japan, 1975, pp.33-34 (in Japanese)